Simultaneous imaging of total cerebral hemoglobin concentration, oxygenation, and blood flow during functional activation

Andrew K. Dunn, Anna Devor, Hayrunnisa Bolay,* Mark L. Andermann, Michael A. Moskowitz,* Anders M. Dale, and David A. Boas

Athinoula A. Martinos Center, Massachusetts General Hospital, 149 13th Street, Charlestown, Massachusetts 02129

Received August 12, 2002

A simple instrument is demonstrated for high-resolution simultaneous imaging of total hemoglobin concentration and oxygenation and blood flow in the brain by combining rapid multiwavelength imaging with laser speckle contrast imaging. The instrument was used to image changes in oxyhemoglobin and deoxyhemoglobin and blood flow during cortical spreading depression and single whisker stimulation in rats through a thinned skull. The ability to image blood flow and hemoglobin concentration changes simultaneously with high resolution will permit detailed quantitative analysis of the spatiotemporal hemodynamics of functional brain activation, including imaging of oxygen metabolism. This is of significance to the neuroscience community and will lead to a better understanding of the interrelationship of neural, metabolic, and hemodynamic processes in normal and diseased brains.

OCIS codes: 170.0110, 170.3880, 170.5380.

Optical imaging of functional brain activation based on intrinsic signals has revealed new insights into the functional representations of areas such as the visual[1] and somatosensory[2] cortices. In most intrinsic optical imaging approaches the exposed cortex is illuminated with a single wavelength, and changes in the reflected light are imaged onto a CCD camera. Intrinsic optical imaging is sensitive primarily to changes in total hemoglobin concentration and oxygenation that result from increases in neuronal activity as the result of a functional stimulus. Although the spatial organization of functional activations can be qualitatively mapped with single-wavelength intrinsic optical imaging, no quantitative information about total hemoglobin (HbT) concentration, oxygenation, or blood flow is obtained. To quantify changes in oxyhemoglobin (HbO) and deoxyhemoglobin (Hb), one must use multiple wavelengths. Previous efforts have included spectroscopic measurements at a single spatial location[3] and measurements where the reflected light from a one-dimensional slit on the tissue is dispersed by a diffraction grating onto a CCD, yielding one spatial dimension and one spectral dimension.[4] High-resolution quantitative two-dimensional imaging of the spatiotemporal dynamics of HbT concentration changes and oxygenation has not previously been demonstrated for functional activation of the cortex.

In addition to hemoglobin changes, cerebral blood flow (CBF) changes resulting from functional activation are an important component of the hemodynamic response. Laser Doppler flowmetry is typically used for blood flow monitoring and provides high-temporal-resolution measurements of relative blood flow changes at a single point on the cortex, yet no spatial information is obtained. Although scanning laser Doppler systems provide some spatial resolution, their temporal resolution is insufficient for imaging the response to most functional stimuli because of the need for scanning. One can, however, use laser speckle contrast imaging[5] to image CBF changes[6] dynamically without the need for scanning. Laser speckle contrast imaging has been used to image blood flow in migraine headache,[7] the retina,[8] and skin.[9]

The combination of speckle and spectroscopic imaging will aid in furthering the understanding of the complex coupling between the underlying neuronal and metabolic activity and the observed hemodynamic response as well as lead to greater insight into disease mechanisms in the brain, which can then result in new treatments.

In this Letter we describe a single instrument capable of simultaneously imaging both CBF and HbT concentration and oxygenation changes in the brain through a thinned skull preparation. Blood flow is imaged by use of laser speckle contrast imaging, and a six-wavelength filter wheel is used to acquire spectral images for calculation of HbO and Hb images. The instrument is depicted in Fig. 1. An expanded diode laser ($\lambda = 785$ nm) illuminates the cortex at an angle of approximately 30°, and the resulting speckle pattern is imaged onto a cooled 12-bit CCD camera. For multiwavelength imaging a mercury xenon arc lamp is directed through a six-position filter wheel and is coupled

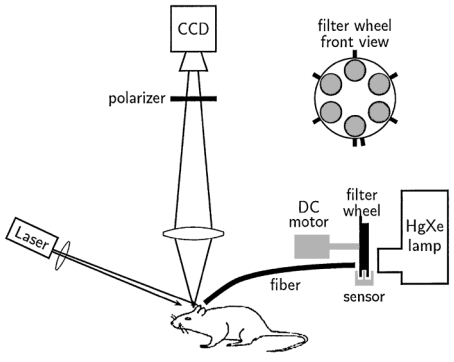

Fig. 1. Geometry for simultaneous laser speckle contrast imaging of blood flow and spectral imaging of hemoglobin oxygenation.

0146-9592/03/010028-03$15.00/0

into a 12-mm fiber bundle that illuminates the cortex. The filter wheel is mounted on a dc motor and is operated continuously at approximately 3 revolutions/s, resulting in a frame rate of ~18 Hz. A radial extension is attached to the filter wheel at each filter position, and, as the filter wheel rotates, each extension passes through an optical sensor, providing a trigger signal for the camera at each filter position. In addition, a second extension attached to the filter wheel at one of the filter positions serves as a reference for the other filter positions. The output of the sensors, as well as a signal from the CCD indicating when an image is acquired, is recorded by a separate computer. These timing signals are necessary to account for the fact that the camera occasionally misses a trigger signal from the filter wheel, with the result that the order of acquired images can vary slightly. Software was written to analyze the timing signals to determine the filter position and time of acquisition for each image. For interleaved spectral and speckle imaging, one of the filter positions is blocked, and the trigger signal for that filter position is used to switch the diode laser on for approximately 5 ms. Therefore, five spectral images and one speckle image are acquired during interleaved operation. Since images at each filter position are not acquired simultaneously, the time series for each set of images was interpolated onto a common time base.

The filters were 10-nm bandpass filters centered at wavelengths of 560, 570, 580, 590, 600, and 610 nm. The modified Beer–Lambert law was used to convert the spectral images to images of HbO and Hb, $\Delta A(\lambda) = \sum \epsilon_i(\lambda)\Delta C_i D_a(\lambda)$, where $\Delta A = \log(R_0/R)$ is the change in attenuation, R and R_0 are the reflectance during activation and baseline, respectively, and ϵ_i and ΔC_i are the molar extinction coefficient and concentration changes of the ith chromophore, respectively. $D_a(\lambda)$ is the differential path-length factor that accounts for the different optical path lengths through the tissue that result from the wavelength dependence of the scattering and absorption coefficients and was generated from Monte Carlo simulations that included the geometry of the imaging system as described by Kohl *et al.*[3] HbO and Hb are the only chormophores of significance, and scattering was assumed to be constant over the wavelength range 560–610 nm. Other chromophores such as cytochrome oxidase and water contribute insignificantly to the absorption spectrum in this wavelength range. We generated relative blood flow images by first converting speckle contrast images to images of intensity autocorrelation decay times. The decay time is assumed to be inversely proportional to flow velocity.[10] We then generated relative flow images by taking the ratio of a flow image to a reference baseline flow image.[6]

To demonstrate the utility of the instrument for simultaneous imaging of cerebral HbT concentration, oxygenation, and blood flow, we used cortical spreading depression (CSD) and whisker stimulation in rats. CSD is characterized by slowly propagating (2–5-mm/min) waves of neuronal depolarization and is important in pathophysiologic conditions such as migraine and ischemia.[11] Associated with the neuronal changes during CSD are large transient changes in CBF and cerebral blood volume.[12] Single-wavelength intrinsic optical imaging has been used to image reflectance changes during CSD, but no technique has made possible simultaneous imaging of blood flow and oxygenation changes during CSD, which could better elucidate the metabolic processes involved.

The rat whisker barrel cortex is a well-characterized model system for studying functional brain activation. Each whisker is mapped in a one-to-one fashion to clusters of neurons approximately 200 μm in diameter, called barrels, on the contralateral somatosensory cortex. Intrinsic optical imaging is one of the established techniques for studying the functional response of the cortex to whisker stimulation, but to our knowledge no technique has previously produced quantitative images of the blood flow and hemoglobin oxygenation response to whisker stimulation.

CSD was induced by pinprick to the exposed cortex, and images were acquired through a 6 mm × 6 mm cranial window. The details of the preparation were described elsewhere.[6,7] The fractional changes in HbO and Hb concentrations as well as CBF are illustrated in Fig. 2 during a single CSD, and the time course of the changes is also plotted for the two regions indicated in Fig. 2a. The three images show the spatial changes in HbO, Hb, and blood flow 1 min following induction of CSD in the upper left portion of the imaged area. The large increase in CBF and cerebral blood volume typically observed in CSD is seen propagating from top to bottom with a speed of ~4.2 mm/min, which is consistent with previous reports.[11] Changes in HbO and Hb in individual surface vessels can be resolved. In particular, a significant decrease in Hb is observed along a single vessel ahead of the propagating wave of hyperemia, indicating that that particular vessel is likely a draining vein. In addition, we calculated the change in scattering during CSD and found a slight increase (~10%) in the reduced scattering coefficient, μ_s'. However, we did not observe a biphasic change in μ_s' as reported by Kohl *et al.* during CSD with noninvasive near-infrared spectroscopy.[13] The reason for the discrepancy most likely is due to the fact that

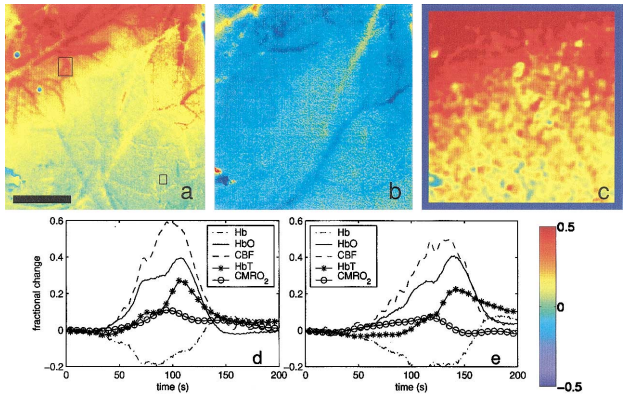

Fig. 2. Changes in a, HbO, b, Hb, and c, CBF 1 min after induction of CSD. The boxes in a indicate the regions of interest for the time courses. d, Top left region, e, lower region. Scale bar, 1 mm.

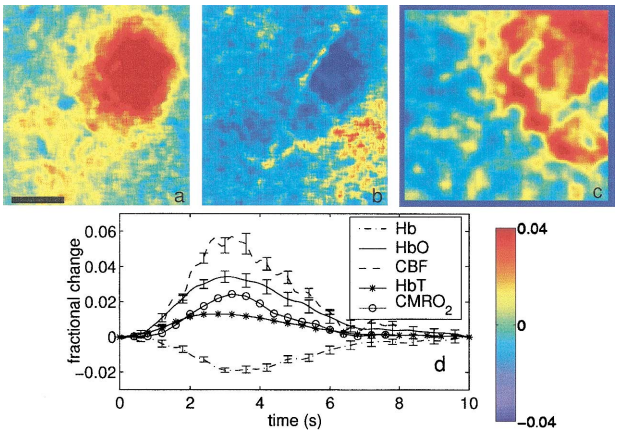

Fig. 3. Images of changes in a, HbO, b, Hb, and c, CBF following single whisker deflection. The time course, d, is the average response over the activated region. Scale bar, 0.5 mm.

near-infrared spectroscopy measurements will be more sensitive to scattering changes since photon path lengths within the tissue are considerably longer for near-infrared spectroscopy measurements than for our instrument.

The cerebral metabolic rate of oxygen, $CMRO_2$, can be calculated from the fractional changes in CBF, Hb, and HbT[14] (HbT = HbO + Hb), $1 + \Delta CMRO_2/CMRO_2 = (1 + \Delta CBF/CBF_0)(1 + \gamma_R \Delta Hb/Hb_0)(1 + \gamma_T \Delta HbT/HbT_0)^{-1}$, where γ_R and γ_T are vascular weighting constants[14] and were assumed to be 1. Note that the peak change in CBF is approximately four times greater than the peak change in $CMRO_2$, suggesting an uncoupling similar to that observed for other brain activations.[15] It is also interesting to note that $CMRO_2$ reaches a plateau near a single peak, whereas CBF, HbO, and HbT show a secondary increase, suggesting a delayed stress relaxation in the vessels.[16]

In addition to the large hemodynamic changes such as those that occur during CSD, the instrument can also image significantly smaller changes in hemodynamics such as those from whisker stimulation. Figure 3 illustrates the fractional changes that occur during stimulation of a single whisker in a rat. The rat was prepared in the same manner as the CSD measurements, and a single whisker was deflected for 2 s at a frequency of 5 Hz by a computer-controlled stimulator. Spectral and speckle image sets were acquired in separate whisker deflection trials rather than interleaved because the hemodynamic response and duration of the response are approximately ten times smaller compared with CSD. A total of 60 trials, with 20 s of rest between trials, were averaged for both speckle and spectral image sets. Activation images of HbO, Hb, and CBF are shown in Fig. 3 and were taken as the ratio of the response integrated over 3–4 s following stimulus to baseline (1 s prestimulus). A localized region of activation corresponding to a single whisker barrel region is observed, and the spatial extent of the CBF response is less well localized than the hemoglobin changes. The time courses of the changes in HbO, Hb, CBF, $CMRO_2$, and HbT in the region of activation are also shown. Note that the peak response and recovery of Hb are slightly delayed relative to the increase in the other hemodynamic parameters, consistent with the observations of others,[4,17] and that the ratio of the CBF and $CMRO_2$ change is ~3, in agreement with others.[14]

The instrument described in this Letter has the ability to reveal important new insights into the spatiotemporal dynamics of functional brain activation. Other techniques such as single-wavelength intrinsic optical imaging lack the ability to quantify both spatial and temporal hemoglobin oxygenation changes. When this instrument is coupled with speckle contrast imaging of CBF, the full set of hemodynamic parameters can be imaged with high spatial and temporal resolution, allowing oxygen metabolism dynamics to be investigated in great detail. Another significant advantage of this system is its relative simplicity and ease of implementation.

This work was supported by the National Institutes of Health (5K25NS041291, R01EB00790-01A2, P41-RR14075), the Whitaker Foundation, and the Mental Illness and Neuroscience Discovery Institute. The authors thank Eric Bennett for assistance in construction of the microscope. A. Dunn's e-mail address is adunn@nmr.mgh.harvard.edu.

*Stroke and Neurovascular Regulation Laboratory.

References

1. D. Ts'o, R. Frostig, E. Lieke, and A. Grinvald, Science **249,** 417 (1990).
2. T. Woolsey, C. Rovainen, S. Cox, M. Henegar, G. Liang, D. Liu, Y. Moskalenko, J. Sui, and L. Wei, Cereb. Cortex **6,** 647 (1996).
3. M. Kohl, U. Lindauer, G. Royl, M. Kuhl, L. Gold, A. Villringer, and U. Dirnagl, Phys. Med. Biol. **45,** 3749 (2000).
4. D. Malonek and A. Grinvald, Science **272,** 551 (1996).
5. J. Briers, Physiol. Meas. **22,** R35 (2001).
6. A. Dunn, H. Bolay, M. Moskowitz, and D. Boas, J. Cereb. Blood Flow Metab. **21,** 195 (2001).
7. H. Bolay, U. Reuter, A. Dunn, Z. Huang, D. Boas, and M. Moskowitz, Nature Med. **8,** 136 (2002).
8. Y. Tamaki, M. Araie, E. Kawamoto, S. Eguchi, and H. Fuji, Invest. Ophthalmol. Vis. Sci. **35,** 3825 (1994).
9. J. Briers and S. Webster, J. Biomed. Opt. **1,** 174 (1996).
10. R. Bonner and R. Nossal, Appl. Opt. **20,** 2097 (1981).
11. M. Lauritzen, Cephalalgia **21,** 757 (2001).
12. A. O'Farrell, D. Rex, A. Muthialu, N. Pouratian, G. Wong, A. Cannestra, J. Chen, and A. Toga, Neuroreport **11,** 2121 (2000).
13. M. Kohl, U. Lindauer, U. Dirnagl, and A. Villringer, Opt. Lett. **23,** 555 (1998).
14. M. Jones, J. Berwick, D. Johnston, and J. Mayhew, Neuroimage **13,** 1002 (2001).
15. P. Fox and M. Raichle, Proc. Natl. Acad. Sci. USA **83,** 1140 (1986).
16. J. Mandeville, J. Marota, C. Ayata, G. Zaharchuk, M. Moskowitz, B. Rosen, and R. Weisskoff, J. Cereb. Blood Flow Metab. **19,** 679 (1999).
17. H. Obrig, C. Hirth, J. Junge-Hulsing, C. Doge, T. Wolf, U. Dirnagl, and A. Villringer, J. Appl. Physiol. **81,** 1174 (1996).